Newly Developed Seismic Resilient Steel Pipe Joint Safeguards: Pipeline Structural Integrity during Severe Geohazard Events

Brent D. Keil[1]; Richard D. Mielke[2]; Fritz Gobler[3]; Gregory Lucier[4]; Gregory C. Sarvanis[5]; Giannoula Chatzopoulou[6]; Dimitris Fappas[7]; and Spyros A. Karamanos[8]

[1]Northwest Pipe Co., Vancouver, WA. Email: BKEIL@nwpipe.com
[2]Northwest Pipe Co., Vancouver, WA. Email: RMIELKE@nwpipe.com
[3]Northwest Pipe Co., Vancouver, WA. Email: fgobler@nwpipe.com
[4]North Carolina State Univ., Raleigh, NC. Email: gwlucier@ncsu.edu
[5]Univ. of Thessaly, Volos, Greece. Email: gsarvan@uth.gr
[6]Univ. of Thessaly, Volos, Greece. Email: gihatzop@uth.gr
[7]Univ. of Thessaly, Volos, Greece. Email: dimitrisfp@gmail.com
[8]Univ. of Thessaly, Volos, Greece. Email: skara@mie.uth.gr

ABSTRACT

The mechanical performance of lap welded joints is essential for safeguarding the structural integrity of steel water pipelines, after a severe earthquake or other geohazard loadings. Over the past 4 years, an extensive experimental project was launched to determine the structural performance of lap welded joints under the most severe ground deformations. The research consisted of full-scale physical experiments, supported, and validated by rigorous numerical finite element simulations. The experimental results have indicated a remarkable strength and deformation capacity of the standard lap welded joints without loss of water containment. In addition questions related to local lap weld joint deformation were elucidated and the corresponding strains developed under extreme tensile or compressive loads at critical locations were quantified, demonstrating the ability of those joints to sustain a significant amount of local strain at critical locations. The latest phase of the research focuses on the behavior, analysis, and design of a new seismic resistant lap welded joint. Results of a series of additional full-scale experiments, supported by finite element numerical simulations, on the mechanical performance of the new lap welded joints under severe structural (axial and bending) loading conditions are presented herein. The new lap weld joint comprises the standard lap weld configuration but contains a small geometric projection introduced at a specific location near the field applied fillet weld. Based on current research results, a modification of the standard lap welded joint is proven to result in consistent buckling of the steel pipe cylinder and not the lap weld joint, during severe or extreme loading. The proposed joint, referred to as “Atlas Seismic Resilient or ATLAS SR-joint”, effectively allows steel pipe to not be limited by the capacity of the standard lap welded joint during strong seismic or geohazard events, and offers an efficient, reliable, yet economical solution for welded joints in steel water pipelines in geohazard areas.

INTRODUCTION

Welded steel water pipelines are usually constructed with lap joints instead of butt-welded joints, due to their lower construction cost, and their successful proven history of use. The welded lap joint consists of a “bell” which is cold-formed at the end of each pipe segment so that the end of the adjacent pipe segment, often referred to as “spigot”, is inserted and welded to the bell through a single or double full-circumferential fillet weld, as shown in **Figure 1**.

Often welded steel pipelines are constructed in geohazard (seismic) areas, where the pipeline may be subjected to severe transient (shaking) and permanent ground-induced actions from fault rupture, liquefaction-induced lateral spreading, soil subsidence, or slope instability (Sarvanis *et al*. 2018). Any of these actions may deform and strain the pipe well beyond the stress limits associated with normal operating conditions, into the inelastic range of the steel material. In those areas, in addition to the pressure design requirements under normal operating conditions, there is a need for safeguarding structural integrity of the pipeline, against severe ground-induced actions. The seismic design framework of water pipelines has been described recently by Karamanos *et al*. (2017a), where the deformation and strain capacity and strength of welded lap joints has been identified as an area of study.

Using advanced finite element simulation tools, a few early attempts to examine the mechanical response of welded lap joints under bending loads have been reported by Karamanos *et al*. (2015, 2017b). More recently, experimental results on lap welded joints under bending loading conditions have been reported by Keil *et al*. (2018), supported by numerical simulations in a companion paper (Chatzopoulou *et al*., 2018). These tests and analyses referred to two welded lap joints of 25.75-inch outside diameter pipes (24 inch nominal), with thickness equal to 0.135in and 0.250in, made of steel grade ASTM A1011 SS GR36 and ASTM A1018 SS GR40, respectively. Additional numerical results, in continuation of the two results reported in the two aforementioned papers, have been presented by Sarvanis *et al*. (2019). The main conclusion from those works is that the standard lap welded joints are capable of sustaining a significant amount of bending deformation while maintaining water containment, whereas the lap weld joint strength is quite close to the strength of the plain pipe.

The present paper builds upon the work presented in the above papers, and reports experimental results of the structural performance of a newly developed seismic resilient steel lap weld joint, referred to as “ATLAS SR-joint”, subjected to bending and axial compression and tension loadings. The concept of the new joint is presented first, with the use of finite element simulations, and subsequently, the results of large-scale experiments are presented in order to verify the capability of the new joint to deform and buckle in a controlled manner, ensuring the strength and deformation capacity of the joint.

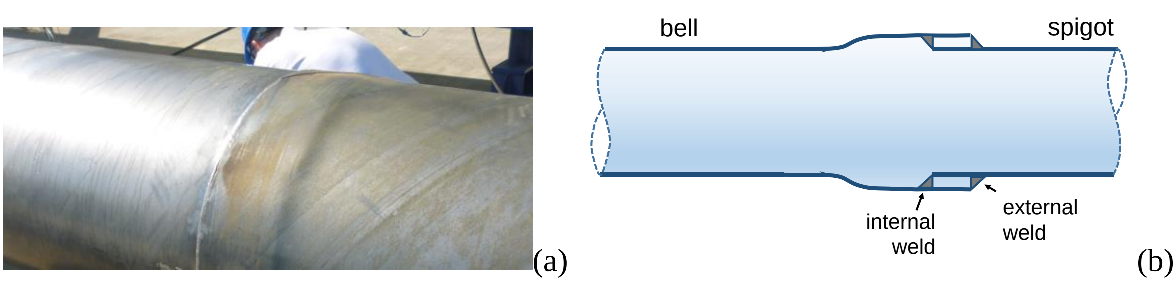

Figure 1. Configuration of lap-welded steel pipe joint.

THE “ATLAS SR-JOINT” CONCEPT

The experimental results reported by Keil *et al*. (2018), and the relevant numerical calculations (Chatzopoulou *et al*., 2018; Sarvanis *et al*., 2019), indicated an excellent structural performance of the welded lap joints. More specifically, the ultimate bending strength of the joints has been found to be more than 80% of the corresponding strength of the plain, unjointed pipe. Furthermore, the joints were able to bend at large values of curvature, well beyond the maximum load, without loss of any water pressure containment. Recent experimental results from axially-compressed lap welded joints (Keil *et al*., 2020), verified the very good performance of those joints in terms of strength and their deformation capacity.

In the above-mentioned tests, despite the excellent performance of the lap welded joints, several specimens exhibited buckling at the bell and through the field applied fillet weld, which may cause some concerns on the capability of the joints to sustain the deformation imposed by severe ground-induced action. The bell is made by cold expansion, which introduces work hardening and residual stresses, and because of its geometry, it is associated with higher local stresses than the pipe cylinder. This concern, although not justified by the recent experimental data, has motivated several welded joint concepts, such as the Enduro Bell (McPherson *et al*., 2016) and the JFE joint (Nakazono *et al*., 2019). However, both solutions may be neither simple nor economical to manufacture or install.

Numerical calculations with finite element models have shown that the location of the buckle is quite sensitive to small initial geometric projection at the pipe wall Therefore, it may be possible to impose a small initial geometric change at the spigot, near the weld, in order to enforce the buckle to occur in the spigot, and prevent the buckle to occur at the bell and avoid including the field weld in the buckle, as shown in **Figure 2**. On the other hand, the above geometric projection, herein referred to as "seismic projection", has to satisfy two main requirements: (a) it should be large enough to ensure that buckling would occur at the projection in the spigot location and not in the bell, and simultaneously, (b) it should be small enough, so that the structural strength of the joint is not significantly affected. To satisfy both requirements, an optimum size of the initial geometric change should be defined, and this requires a detailed finite element analysis, described in the next section of the paper. From the pipe manufacturing point-of-view, this projection can be easily introduced within the normal fabrication process of the pipe. The lap welded joint equipped with the above "seismic projection" will be referred to as the "ATLAS SR™ or Atlas Seismic Resilient™ joint" (patent pending).

The present paper offers a thorough investigation of the ATLAS SR-joint concept under consideration, by performing a large number of numerical simulations. An initial geometric perturbation (seismic projection) is imposed at the spigot, to enforce the formation of a buckling pattern at the spigot, and prevent the occurrence of a buckle at the bell or at the field weld location while not affecting the overall structural strength of the welded lap joint.

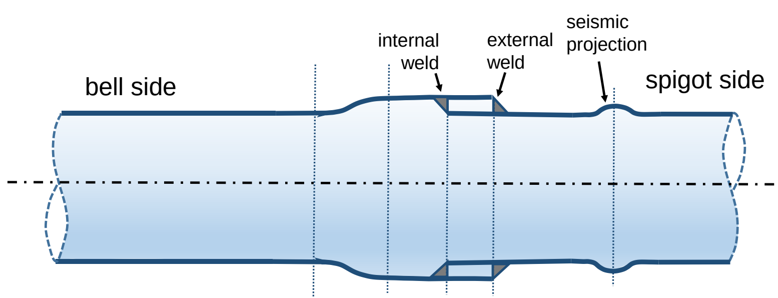

Figure 2. Lap welded joint equipped with the artificial "seismic projection"; ALTAS SR-joint concept (not to scale).

NUMERICAL ANALYSIS OF THE "ATLAS SR-JOINT"

A finite element model has been developed in ABAQUS/Standard to simulate joint behavior, including this "seismic projection". The model consists of four (4) main parts, a pipe with a bell configuration, a pipe with a projection at a specific distance from the end cross section (spigot), and the weld, as shown in **Figure 3a**. The model employs four-node, reduced-integration shell finite elements, referred to as S4R, for the two pipes and 8-node solid "brick" elements for the fillet weld(s). The total length of the model is 120 inches. The gap size between the bell and the spigot is assumed constant around the pipe and is equal to 0.05 inch, which is within the AWWA C200 requirements. The reader is referred to the recent publications by Chatzopoulou *et al*. (2018) and Sarvanis *et al*. (2019) for more information on the model.

Initially, bell expansion is simulated by expanding the pipe end, using an appropriate mandrel, simulated as a rigid body that moves outwards at the radial direction, as shown in **Figure 3b**. Subsequently, the "seismic projection" is introduced at the spigot by expanding the pipe at a specific location, using a mandrel of appropriate geometry, also modelled as rigid body, which moves outwards in the radial direction, as shown in **Figure 3c**. In **Figure 4** the mesh of the numerical model is presented.

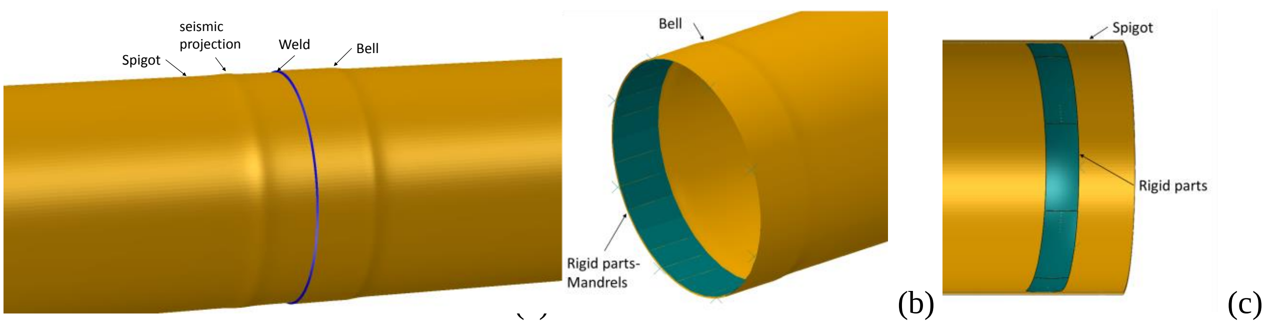

Figure 3. Finite element model of the welded lap joint; geometry of the double-welded area of the joint.

Following the formation of "seismic projection" at the spigot, the spigot and the bell are connected with the weld parts using appropriate kinematic constraints that ensures the continuity of the geometry. Appropriate kinematic constraints are employed as follows; a "tie" is used to connect the spigot and the welds, and a "rough contact" with "no separation" is employed to connect the bell with the welds. Two reference points are also considered, located at each end of the model. Each reference node is coupled in all six degrees of freedom with the degrees of freedom of end-section nodes of the pipe specimen, in order to apply the necessary boundary conditions. In the case of pure bending, the same amount of rotation (of opposite sign) is imposed at the two reference nodes. For compressive loading, the axial displacement is applied at the reference node of the bell part, while the end section of the spigot part remains fixed.

A major parameter to be determined in the ATLAS SR-joint is the amplitude of the "seismic projection". As mentioned above, the "seismic projection" should be large enough to ensure that buckling would occur at the spigot location, and simultaneously, should be small enough, so that the structural strength of the joint is not significantly affected. To quantify this, the following criterion is adopted in the present analysis: the axial strains developed at the spigot due to the "seismic projection" forming should be lower than the axial residual strains at the bell pipe.

Following an extensive numerical parametric study, the optimum amplitude of this projection has been found equal to less than one of pipe wall thickness for the thin-walled pipe (0.135-inch thick), and the thick-walled pipe (0.250-inch thick), respectively. In other words, the amplitude of this initial projection should be somewhat less than (or equal to) the pipe wall thickness.

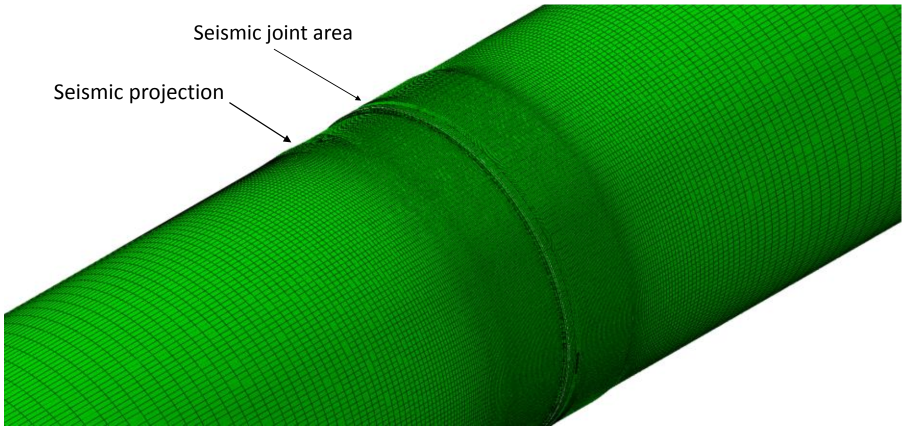

Figure 4. Finite element mesh of the numerical model for the ATLAS SR-joint.

DESCRIPTION OF EXPERIMENTAL PROCEDURE

Large-scale physical experiments to verify the above concept were performed in the facilities of Northwest Pipe Co., at Adelanto plant, California, on pipes with outer dimeter equal to 25.75 inches (0.654 m) and two thicknesses: 0.135 inches (3.429 mm) and 0.250 inches (6.35 mm). The experimental setup for bending tests is shown in **Figure 5**, presented in more detail by Keil *et al*. (2018). It consists of a rectangular self-reacting frame with dimensions approximately 55 feet × 15 feet (16.5 m × 4.5 m), the 50 foot (15 m) pipe specimen, two actuators of total load capacity 45 kips (200 kN) and two metal straps at the intermediate supports. The actuators and the metal straps are pinned at their both ends, in order to allow the pipe at those locations to rotate freely. The distance between the two straps, is actually the length of constant bending moment, equal to about 10 feet (3 m.

The setup for the axial experiments, shown in **Figure 6**, consists of two very stiff horizontal plates connected with four (4) vertical hydraulic actuators with total capacity more than 1573 kips (7,000 kN). The specimens used in axial compression experiments have a total length of 57 inches (1.447 m). In all specimens, pressure has been applied first at 40% of yield pressure ($p_Y = 2\sigma_Y t/D$), and subsequently, keeping the pressure level constant, bending or axial loading has been applied using the hydraulic actuators. In both cases, the load has been recorded together with pipe deflection at critical points around the lap joints. Moreover, local strains, at the area of the lap joints, have been measured at both bell and spigot side of the pipe specimen using strain gauges. In total, eleven (11) experiments have been performed, considering all possible weld patterns of lap joints (double, single-internal and single-external). Six (6) specimens have been tested under monotonically-increasing four-point bending, four (4) specimens were subjected to monotonically-increasing uniform axial compression, and one (1) specimen has been tested under axial cyclic loading. More details on the specimens are summarized in **Table 1**.

EXPERIMENTAL RESULTS

The experimental results are presented in **Figure 7** in terms of force-displacement diagrams of specimens B3-ASI-SR and AC1-AD-SR. In that figure the corresponding tests of a regular lap-joint are also presented for comparison purposes. The comparison of ultimate load capacity of the seismic joint and that of the corresponding regular joint indicates that the seismic joint has a lower yet very comparable strength. This means that the presence of the "seismic projection" reduces only slightly the ultimate load capacity of the lap welded joint under consideration. The same trend was observed in all tests presented in **Table 2**. In **Figure 8** and **Figure 9** the position of local buckling for all seismic-joints, bending and axial, is depicted, for all tests performed. In all cases, local buckling occurred at the spigot side of the connection, verifying the proper function of the "seismic joint" concept.

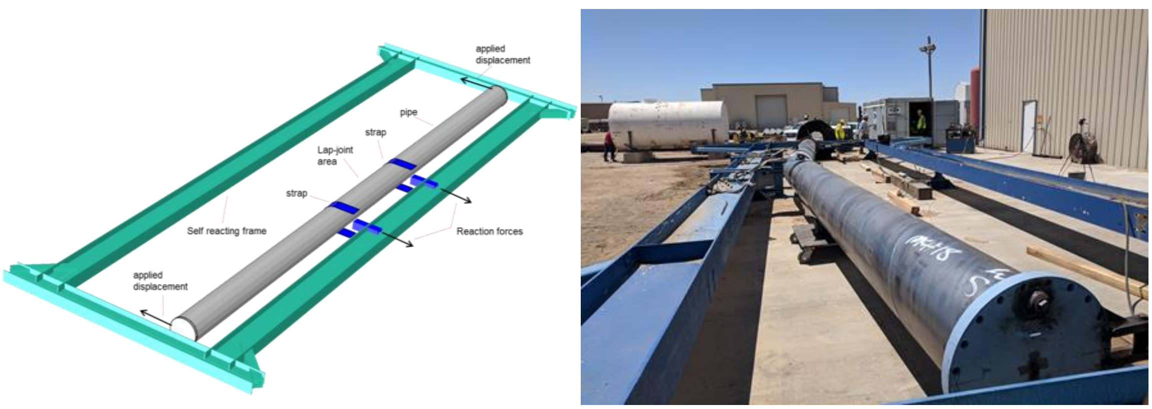

Figure 5. Experimental setup for bending tests.

In **Figure 10** and **Figure 11**, tensile and compressive strains measured at specific locations of specimens B6-BSI-SR and AC1-AD-SR are plotted in terms of the applied displacement. The experimental results indicate that the ATLAS SR-joints under consideration are capable of sustaining significant amount of local strain without loss of pressure containment. In specimen B6-BSI-SR, subjected to bending, the measurements of the three strain gages 7, 8 and 9, all three located at the bell side, shown in **Figure 10**a, indicate a low level of strain throughout the deformation history. Similarly, very small values of strain occur at the vicinity of the weld at strain gages 5 and 6, shown in **Figure 10**b. On the other hand, strain gages 3 (oriented longitudinally) and 4 (oriented in the hoop direction), both located at the crest of the "seismic projection", recorded very high values of strain at the early stages of loading. Unfortunately, both strain gages "failed" when they disbonded at strain equal to 2% (**Figure 10**b), due to the severe local folding of the pipe wall at this location. Finally, two strain gages have been placed at the tension side of the bent specimen, one near the weld (strain gage 1) and one at the crest of the "seismic projection". The former exhibited a tensile response up to 1.6% (before gage "failure"), shown in **Figure 10**c, whereas the latter recorded initially a compressive response (due to straightening of the "seismic projection"), followed by a tensile response, up to 0.8% strain at the end of the test.

In axially-loaded specimen **Figure 11**a, the three strain gages placed at location 1, measured a low level of strain (below 0.05%). This was an expected result, considering that at this location no buckle occurred, and deformations were rather small. The maximum strain measured by the strain gages at location 2, near the weld, is nearly 1% (compressive) and corresponds to the displacement of maximum load. Beyond this load, the area is unstrained and the measured strain decrease. Finally, the strain gages at location 3 (longitudinal direction) exhibit significant deformations due to progressive severe folding of the "seismic projection". The main conclusion from those tests is that the presence of the "seismic projection" triggers the formation of local buckling at the spigot of the lap welded joint away from the weld, whereas the bell area remains practically undeformed.

Table 1. List of specimens.

<table>
<tr><th>loading</th><th>specimen</th><th>weld details</th><th>thickness (in)</th><th>D/t</th><th>pressure (psi)</th></tr>
<tr><td rowspan="6">Bending</td><td>B1-AD-SR</td><td>double weld</td><td rowspan="3">0.250</td><td rowspan="3">103</td><td rowspan="3">325</td></tr>
<tr><td>B2-ASO-SR</td><td>single (outside) weld</td></tr>
<tr><td>B3-ASI-SR</td><td>single (inside) weld</td></tr>
<tr><td>B4- BD-SR</td><td>double weld</td><td rowspan="3">0.135</td><td rowspan="3">191</td><td rowspan="3">170</td></tr>
<tr><td>B5-BSO-SR</td><td>single (outside) weld</td></tr>
<tr><td>B6-BSI-SR</td><td>single (inside) weld</td></tr>
<tr><td rowspan="4">Axial Compression</td><td>AC1- AD-SR</td><td>double weld</td><td rowspan="2">0.250</td><td rowspan="2">103</td><td rowspan="2">325</td></tr>
<tr><td>AC2-ASO-SR</td><td>single (outside) weld</td></tr>
<tr><td>AC3- BD-SR</td><td>double weld</td><td rowspan="2">0.135</td><td rowspan="2">191</td><td rowspan="2">170</td></tr>
<tr><td>AC4-BSO-SR</td><td>single (outside) weld</td></tr>
<tr><td>Axial Cyclic</td><td>AC5-BD-SR</td><td>double weld</td><td>0.135</td><td>191</td><td>170</td></tr>
</table>

Figure 6. Experimental setup for axial compression tests.

Table 2. Experimental results.

specimen	D/t	maximum load (kips)	displacement at buckling (in)	maximum applied displacement (in)	location of buckling
B1-AD-SR	103	-	-	5.94	spigot
B2-ASO-SR	103	-	-	4.17	spigot
B3-ASI-SR	103	22.6	0.31	4.8	spigot
B4- BD-SR	191	9.1	0.19	6.02	spigot
B5-BSO-SR	191	10.1	0.24	6.18	spigot
B6-BSI-SR	191	9.8	0.15	6.26	spigot
AC1- AD-SR	103	854.3	0.12	8.07	spigot
AC2-ASO-SR	103	870.2	0.09	7.95	spigot
AC3- BD-SR	191	591	0.07	8.62	spigot
AC4-BSO-SR	191	496.4	0.11	7.64	spigot

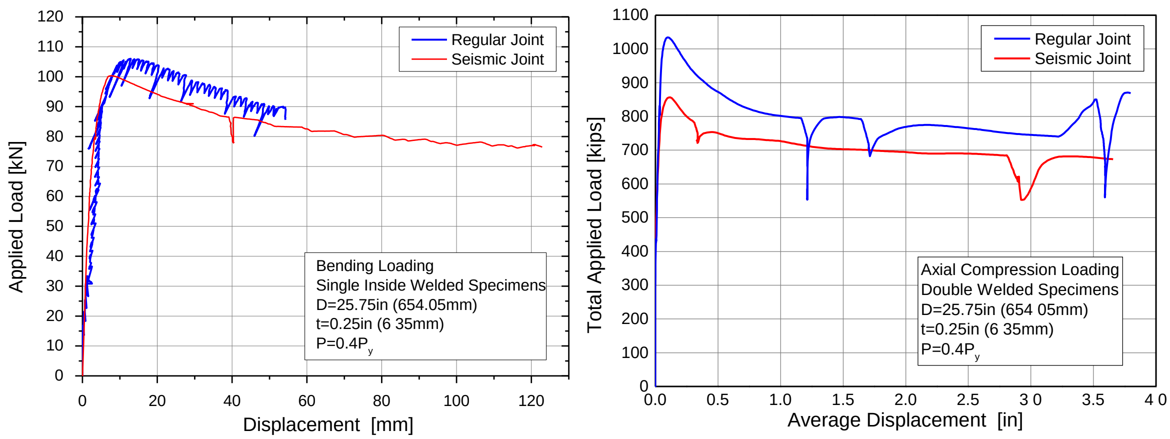

Figure 7. Load-displacement curve under four-point bending of the seismic joint with respect to the regular joint (Keil *et al*. 2018); (a) specimen B3-ASI-SR; (b) specimen AC1-AD-SR.

In **Figure 12** and **Figure 13** the load-displacement curve and the deformed shape of specimen AC5-BD-SR subjected to axial cyclic displacement. The specimen was first compressed up to a stage that local buckling has been significantly developed (0.28 in, (7 mm) of axial displacement). Subsequently, it was subjected to twenty (20) loading cycles, with compressive displacement ranging from approximately 0.69 in (17.5 mm) to zero. During reverse loading to zero displacement, tensile axial load of substantial magnitude was applied. Finally, the specimen was subjected to cyclic loading with maximum and minimum displacement approximately equal to 1.38 in (35 mm) and zero respectively and the specimen lost containment after 5 additional load cycles. Fracture occurred at the crest of the buckle, due to excessive repeated local strain of alternating sign (tension-compression). In total, specimen AC5-BD-SR was capable of undergoing 26 strong loading cycles before losing containment, which is a very satisfactory structural behavior.

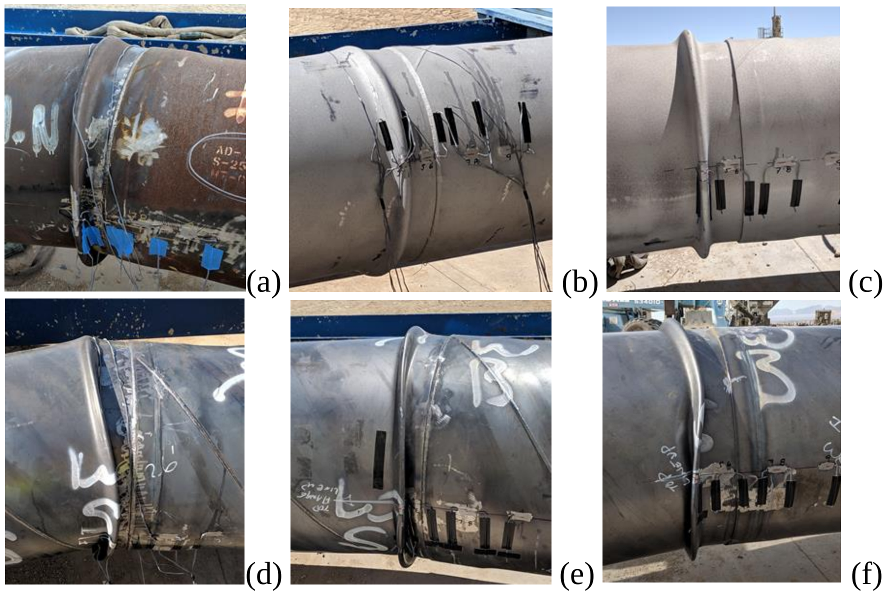

Figure 8. Local buckle configuration in bending experiments; (a) B1-AD-SR, (b) B2-ASO-SR, (c) B3-ASI-SR, (d) B4-BD-SR, (e) B5-BSO-SR, (f) B6-BSI-SR; all specimens buckled at the side of the spigot, where the artificial "seismic projection" was imposed.

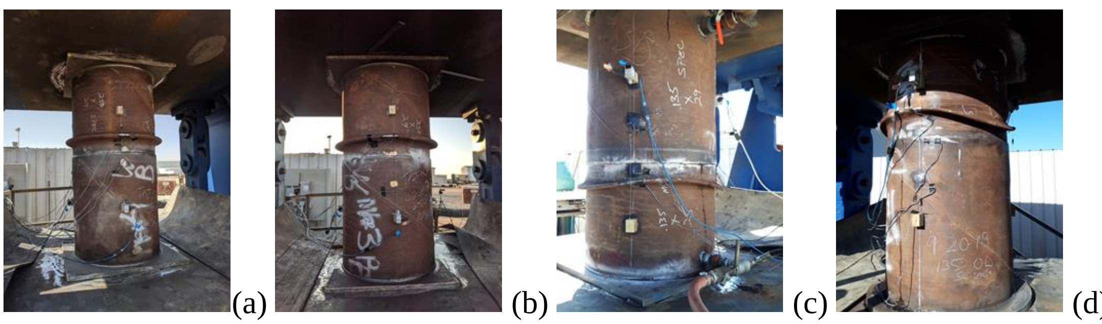

Figure 9. Local buckle configuration in axial compression experiments; (a) AC1-AD-SR, (b) AC2-ASO-SR, (c) AC3-BD-SR, (d) AC4- BSO-SR; all specimens buckled at the spigot side, where the artificial "seismic projection" was imposed.

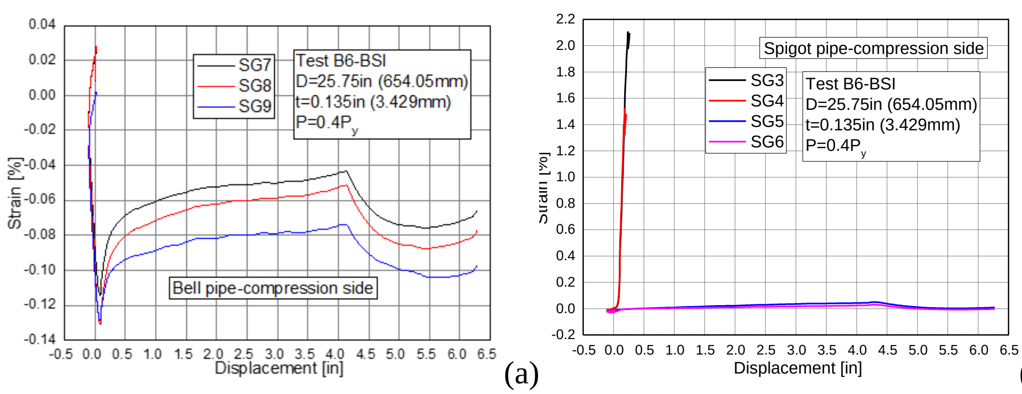

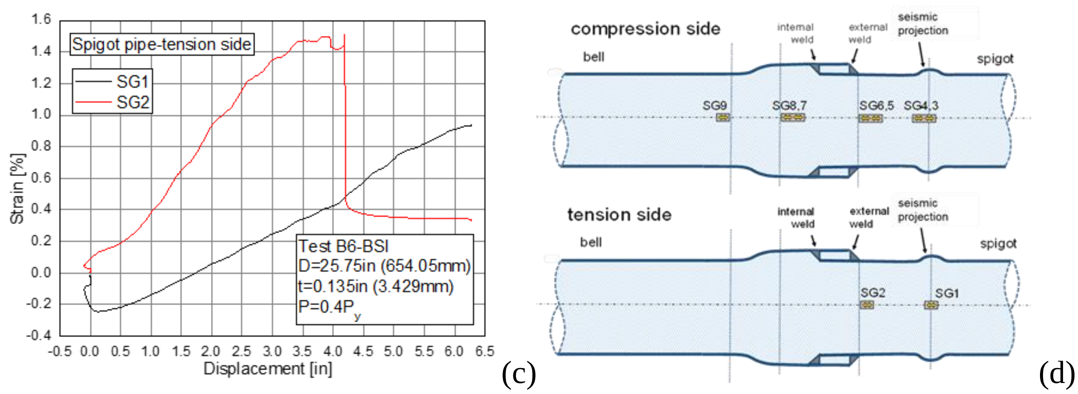

Figure 10. Strains with respect to applied displacements for bending test B6-BSI-SR.

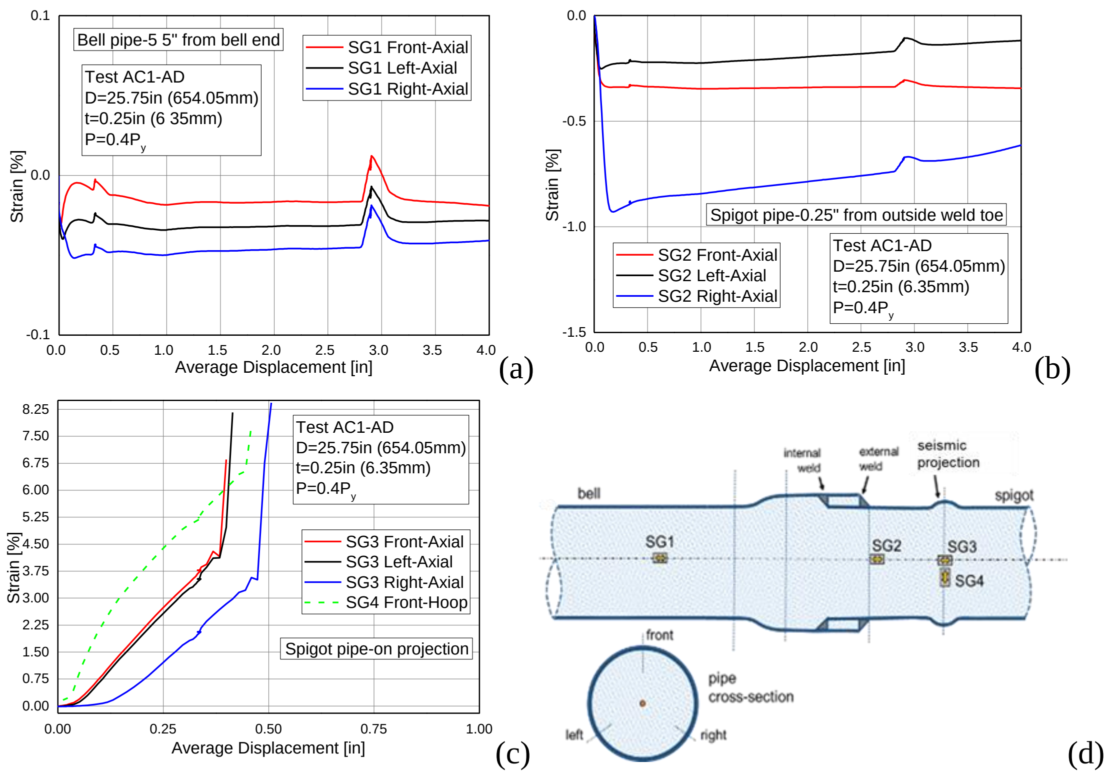

Figure 11. Strains with respect to applied displacements for axially compressed specimen AC1-AD-SR.

The experimental results presented above, demonstrated that the ATLAS SR-joints have been capable of sustaining remarkable bending and axial deformation, under both monotonic and cyclic loading conditions, without any "loss of pressure containment". This is a strong indication that seismic joints can be employed in pipeline applications in seismic areas, where severe permanent ground-induced actions are expected.

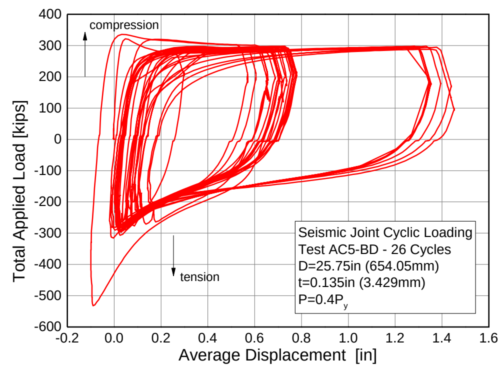

Figure 12. Load-displacement curve of axially-loaded AC5-BD-SR specimen; positive values of axial force correspond to compressive loading.

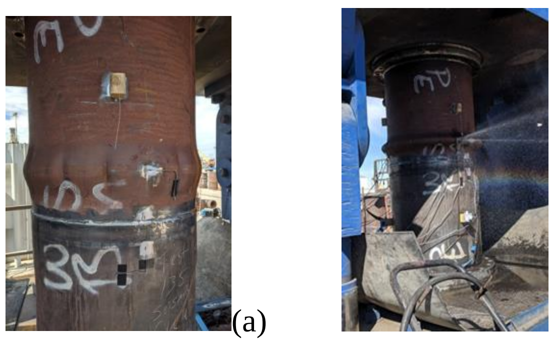

(a) (b)

Figure 13. (a) Deformed shape of axially-loaded AC5-BD-SR specimen; (b) failure of AC5-BD-SR specimen.

CONCLUSIONS

The paper reports experimental results of the structural performance of a newly developed seismic resilient lap weld joint, the "ATLAS SR^{TM}-or Atlas Seismic Resilient^{TM} joint" (patent pending), subjected to bending and axial loading. The joint consists of a standard lap welded joint, equipped with a shop applied seismic projection located at the spigot end near the lap weld. Employing numerical analysis based on rigorous finite element simulations the optimum amplitude of the seismic projection for the tested 24-inch nominal diameter pipe was determined to be slightly below one pipe thickness. With the confirmation of finite element models through physical testing, it will also be possible to scale for pipe diameter and thickness for the seismic projection.

In all experiments, the ATLAS SR-joints have been capable of sustaining remarkable bending and axial deformation, without any "loss of pressure containment". All specimens buckled at the spigot side of the joint, away from the field weld, at the location where this seismic projection has been imposed, while the measured strains at the bell of the joint were quite low. Using this concept, the bell of the lap welded connection and associated field joint weld may no longer be its critical location. Further, the location of a buckling due to extreme movement in the pipe can be predicted. The measured strength and deformation capacity of this joint and its controlled post-buckling deformation at a prescribed location at the spigot, indicate that the "ATLAS SR-joint" constitutes an efficient, reliable and economical solution for lap welded steel pipeline welded joints that increase pipeline safety and resilience in earthquake or other geohazard areas.

REFERENCES

Chatzopoulou, G., Fappas, D., Karamanos, S. A., Keil, B., Mielke R. D., (2018), "Numerical simulation of steel Lap welded pipe joint behavior in seismic conditions.", *ASCE Pipelines Conference*, Toronto, Canada.

Karamanos, S. A., Koritsa, E., Keil, B. and Card, R. J. (2015), "Analysis and behavior of steel pipe welded lap joints in geohazard areas.", *ASCE Pipelines Conference, Paper No. 413*, Baltimore, Maryland, USA.

Karamanos, S. A., Sarvanis, G. C., Keil, B. and Card, R. J. (2017a), "Analysis and Design of Buried Steel Water Pipelines in Seismic Areas.", *ASCE Journal of Pipeline Systems Engineering & Practice*, Vol. 8, Issue 4.

Karamanos, S. A., Koritsa, E., Keil, B. and Pappa, P. (2017b), "Mechanical Response of Steel Pipe Welded Lap Joints in Seismic Areas.", *ASCE Pipelines Conference*, Phoenix, AZ, USA.

Keil, B. D., Gobler, F., Mielke, R. D., Lucier, G., Sarvanis, G. C., and Karamanos, S. A. (2018), "Experimental Results of Steel Lap Welded Pipe Joints in Seismic Conditions", *ASCE Pipelines Conference*, Toronto, Canada.

Keil, B. D., Lucier, G., Mielke, R. D., Fappas D., Sarvanis, G. C., Chatzopoulou, G., Karamanos, S. A. (2020), "Experimental Investigation of Steel Lap Welded Pipe Joint Performance under Severe Axial Loading Conditions in Seismic or Geohazard Areas", *ASCE Pipelines Conference*, San Antonio, Texas.

McPherson, D. L., Duffy, M., Koritsa, E., Karamanos, S. A., Plattsmier, J. R., (2016), "Improving the Performance of Steel Pipe Welded Lap Joints in Geohazard Areas", *ASCE Pipelines Conference*, Kansas City, Missouri.

Nakazono, H., Hasegava, N., Wham, B. P., O'Rourke, T. D., Blake B., (2019), "Innovative Solution to Large Ground Displacement Using Steel Pipe for Crossing Fault", *ASCE Pipelines Conference*, Nashville, Tennessee.

Sarvanis, G. C., Karamanos, S. A., Vazouras, P., Mecozzi, E., Lucci, A., Dakoulas, P. (2018), "Permanent earthquake-induced actions in buried pipelines: Numerical modeling and experimental verification", *Earthquake Engng Struct Dyn*., pp 1–22.

Sarvanis, G. C, Chatzopoulou, G., Fappas, D., Karamanos, S. A., Keil, B., Mielke R. D., Lucier G., (2019), "Finite Element Analysis of Steel Lap Welded Joint Behavior under Severe Seismic Loading Conditions", *ASCE Pipelines Conference*, Nashville, Tennessee.